SUPPLEMENTARY INFORMATION

Competition between reverse water gas shift reaction and methanol synthesis from CO_2: influence of copper particle size

Laura Barberis[1], Amir H. Hakimioun[2], Philipp Plessow[2], Nienke L. Visser[1], Joseph A. Stewart[3], Bart D. Vandegehuchte[3], Felix Studt[2,4] and Petra E. de Jongh[1]*

[1] Materials Chemistry and Catalysis, Debye Institute for Nanomaterials Science, Utrecht University, Universiteitsweg 99, 3584 CG Utrecht, The Netherlands.
[2] Institute of Catalysis Research and Technology, Karlsruhe Institute of Technology, Eggenstein-Leopoldshafen 76344, Germany.
[3] TotalEnergies OneTech Belgium, B-7181 Seneffe, Belgium.
[4] Institute for Chemical Technology and Polymer Chemistry, Karlsruhe Institute of Technology, Karlsruhe 76131, Germany.

*Corresponding author: P.E.deJongh@uu.nl

Table of contents

Section S1: Catalyst Synthesis and structural properties

For a typical impregnation, 1.5 g pristine graphene nanoplates (GNP500) were dried at 170 °C under dynamic vacuum for 2 hours. The vacuum was partially released and impregnated directly afterwards with a 95% pore-filling amount of precursor solution (1-3 M) consisting of $Cu(NO_3)_2 \cdot 3H_2O$ (Acros Organics, ≥99% purity) in 0.1M HNO_3 (Merck, 65% in water). The solution was added dropwise under magnetic stirring. After the addition, the powder was dried at room temperature for 24 hours under dynamic vacuum. To avoid exposure to air, the dried impregnated powder was stored in an Ar-filled glovebox (Mbraun Lab Star Glove Box supplied with pure 5.5 grade Argon, <1 ppm O_2, <1 ppm H_2O). The dried sample, loaded in a plug-flow reactor, was treated following the parameters reported in **Table S1**. The heat treatment was performed under N_2 flow (100 mL min^{-1} g^{-1}), while the reduction step was performed under 10% H_2/N_2 or 20% H_2/N_2 flow (100 mL min^{-1} g^{-1}). After allowing cooling down to room temperature, the obtained sample was transferred to an Ar-filled glovebox. Finally, after characterization of the metallic phase, the catalyst was slowly passivated by exposure to air. The catalysts were pressed and sieved to a grain size of 75-150 μm.

Table S1 (a) Nominal copper weight loading. (b) Temperatures adopted for the heat treatment (T_{HT}) and the reduction (T_R) steps during the synthesis of the catalysts. Surface-averaged Cu particle sizes (in nm) of Cu/C catalysts in the fresh, activated and used state determined by (c) XRD and (d) TEM .

Name	Cu loading (wt. %) [a]	T_{HT} (°C) [b]	T_R (°C) [b]	Fresh Catalysts (nm)		Activated catalysts (nm)		Used catalysts (nm)	
				d_{Cu^0} [c]	$d_s \pm \sigma_{ds}$ [d]	d_{Cu^0} [c]	$d_s \pm \sigma_{ds}$ [d]	d_{Cu^0} [c]	$d_s \pm \sigma_{ds}$ [d]
4.7_Cu/C	5.2	-	250	-	3.9 ± 0.9	-	4.7 ± 1.2	-	4.9 ± 1.3
5.8_Cu/C	9.9	250	200	-	4.3 ± 1.0	-	5.8 ± 1.6	-	5.6 ± 1.5
11.2_Cu/C	9.9	-	250	7.5	8.8 ± 2.6	7.8	11.2 ± 3.6	7.6	11.9 ± 3.7
12.8_Cu/C	9.9	300	200	9.6	8.8 ± 2.8	8	12.8 ± 4.1	7.5	13.3 ± 4.2
19.4_Cu/C	14.1	260	200	12.4	18.0 ± 6.1	16.8	19.4 ± 6.4	16.2	21.2 ± 7.1

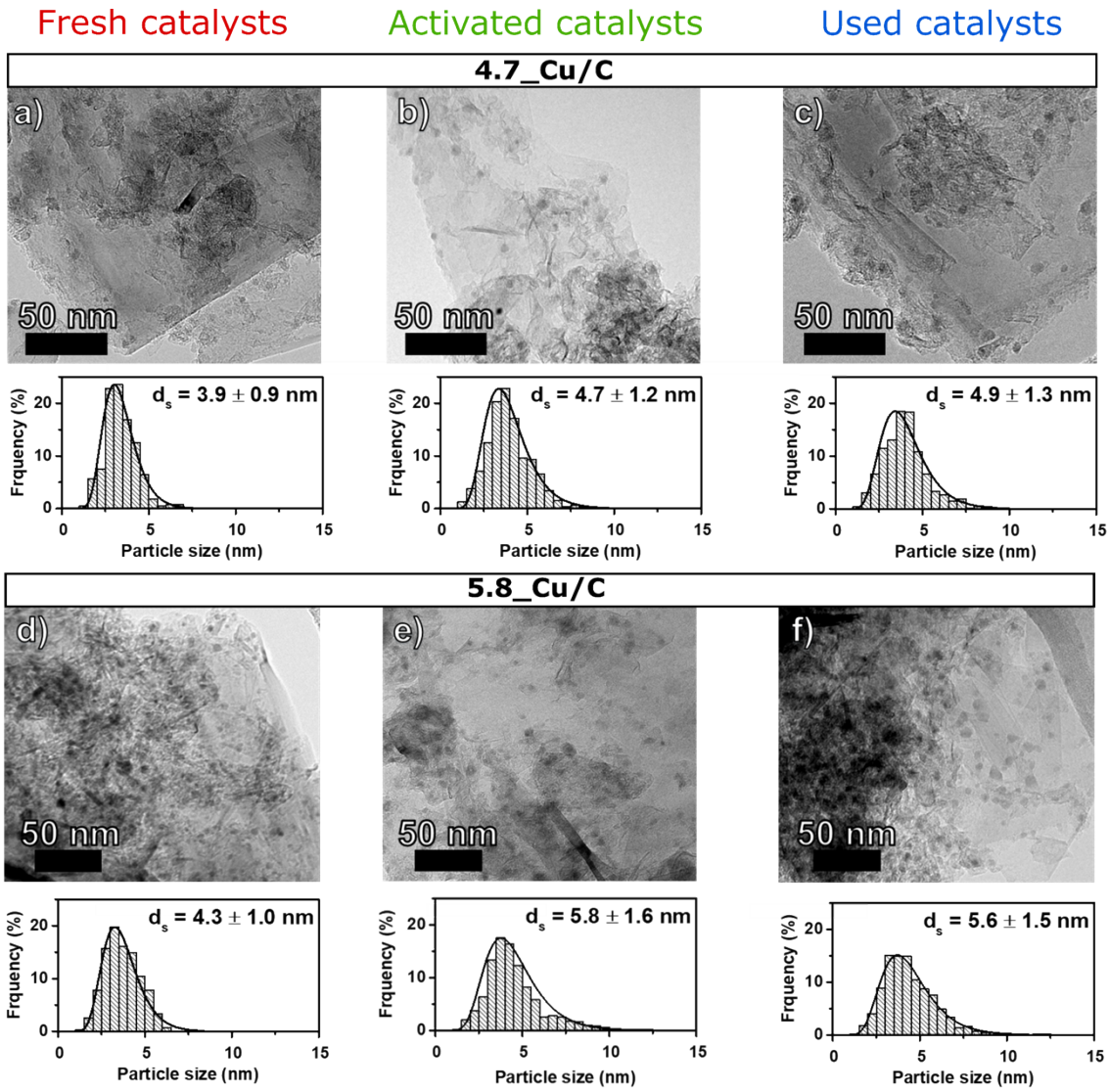
Fresh catalysts
Activated catalysts
Used catalysts
4.7_Cu/C
a)
b)
c)
50 nm
50 nm
50 nm
Frquency (%)
Particle size (nm)
d_s = 3.9 ± 0.9 nm
d_s = 4.7 ± 1.2 nm
d_s = 4.9 ± 1.3 nm
5.8_Cu/C
d)
e)
f)
50 nm
50 nm
50 nm
d_s = 4.3 ± 1.0 nm
d_s = 5.8 ± 1.6 nm
d_s = 5.6 ± 1.5 nm

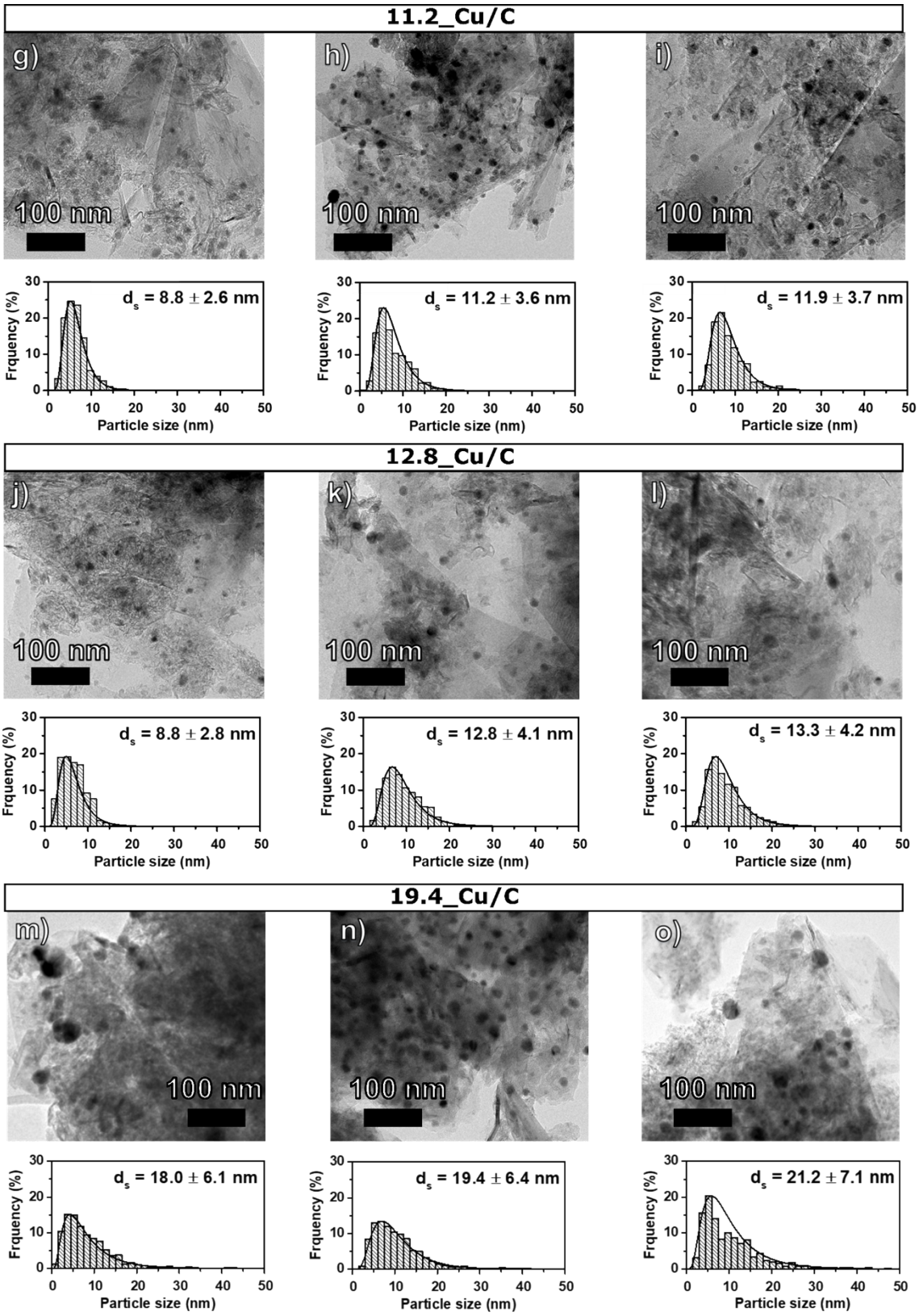

Figure S1 Transmission electron micrographs with corresponding particle size distributions of the Cu/C catalysts in the fresh (a, d, g, j, m), activated (b, e, h, k, n) and used (c, f, I, l, o) state.

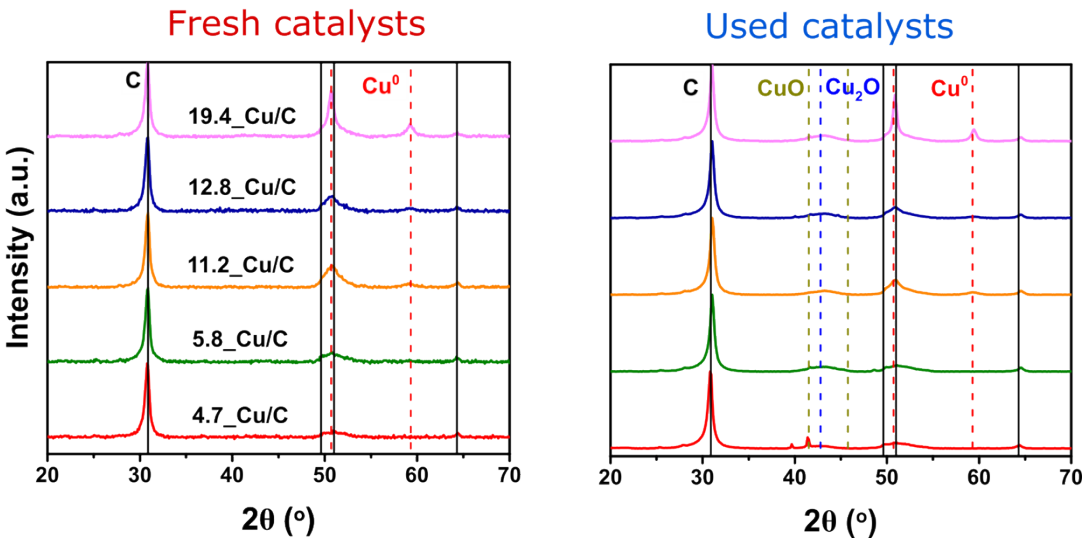

Figure S2 Powder X-ray diffractograms of Cu/C catalysts in the fresh (a) and used (b) state. Diffractograms normalized to the intensity of the carbon (002) diffraction peak at 30.9° 2ϑ and vertically stacked with individual offset.

Section S2: Catalytic performance

The activity of the catalyst was given as CO_2 conversion (X_{CO2}), copper-time yield (CTY) and turnover frequency (TOF). The CO_2 conversion was calculated by the difference in CO_2/Ar ratio between chromatograms taken during reaction through a catalyst-filled reactor and chromatograms taken during reaction through a SiC-filled reference reactor. The TOF was based on CTY and the number of copper surface atoms, according to the equation: $CTY*M_{Cu}/D_{Cu}$. Where CTY is expressed in $mol_{CO2}\ g_{Cu}^{-1}\ s^{-1}$, M_{Cu} is the molar mass of Cu and D_{Cu} is the dispersion of surface Cu atoms. The value of D_{Cu} was calculated as $D_{Cu}=6*V_{Cu}/A_{Cu}*ds$. Therefore, considering the molar volume (V_m) of $7.09*10^{21}\ nm^3$, the molar area of the particles (A_m) of $4.10*10^{22}\ nm^2$ and mean diameter (d_s) of the activated catalyst, as determined by TEM.

The value of the apparent activation energy (E_a) in the Arrhenius model was obtained from the slope of the linear fit through the ln(CTY ($mmol_{CO2}\ g_{Cu}^{-1}\ s^{-1}$)). The pre-exponential factor (A) was obtained in the Arrhenius model from the intercept of the linear fit through the ln(surface-normalized CTY ($mmol_{CO2}\ m^2_{Cu}{}^{-1}\ s^{-1}$)).

The selectivity to methanol or CO was defined as $S_i = 100 * {C_i}/{\sum n * C_i}$ with C_i as the concentration of the product *i* in the effluent gas mixture and *n* the corresponding carbon number. The TOF_{MeOH} and TOF_{CO} were based on the MeOH and CO outflows and the number of copper surface atoms, using the d_s of the activated catalysts (determined by TEM measurements). The values of the apparent activation energy (E_a) in the Arrhenius model for MeOH and CO were obtained from the slope of the linear fit through the ln(CTY ($mmol_{Product}\ g_{Cu}^{-1}\ s^{-1}$)). All calculations were performed considering the data at the end of each isothermal step in order to evaluate the catalysts activity and selectivity under steady-state

conditions.

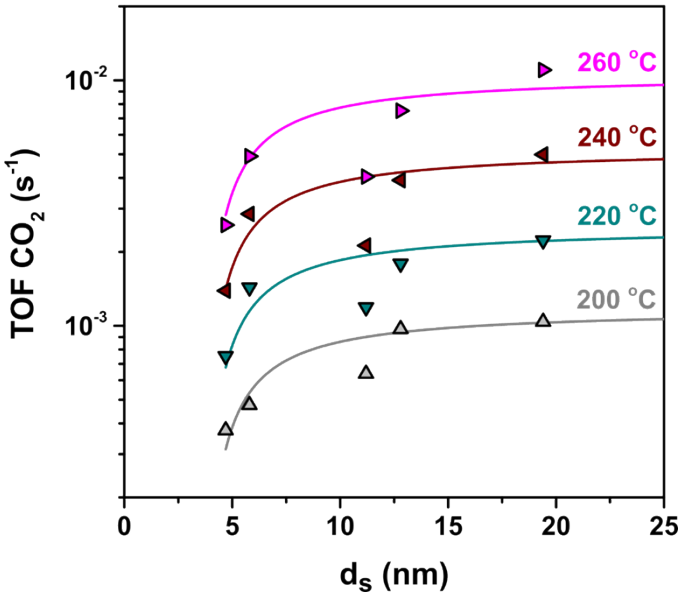

Figure S3 CO_2 TOF as function of Cu particle size at temperature between 200°C and 260°C for the series of Cu/C catalysts. Lines are drawn to guide the eye. Reaction conditions: 40 bar(g), 600 mL min^{-1} g_{Cu}^{-1}, H_2/CO_2/He = 67.5/22.5/10 vol%.

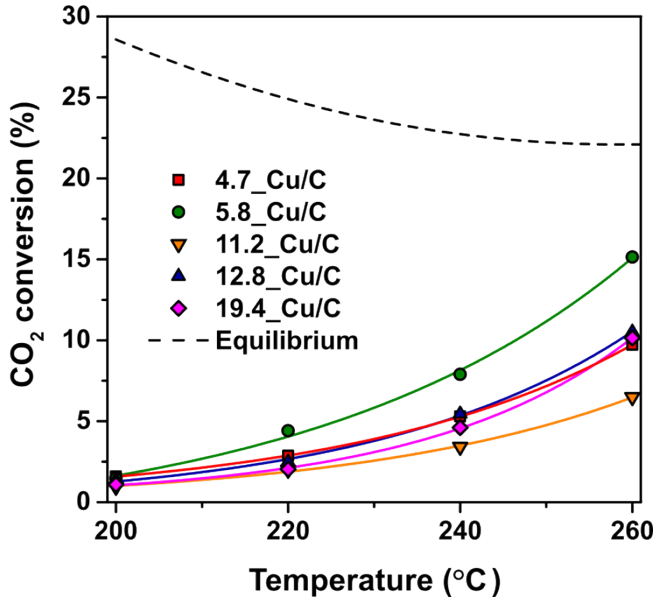

Figure S4 CO_2 conversion as a function of temperature for the Cu/C catalysts with different copper particle size. Equilibrium CO_2 conversion has been reported as well. Reaction conditions: 40 bar(g), 600 mL min^{-1} g_{Cu}^{-1}, H_2/CO_2/He = 67.5/22.5/10 vol%.

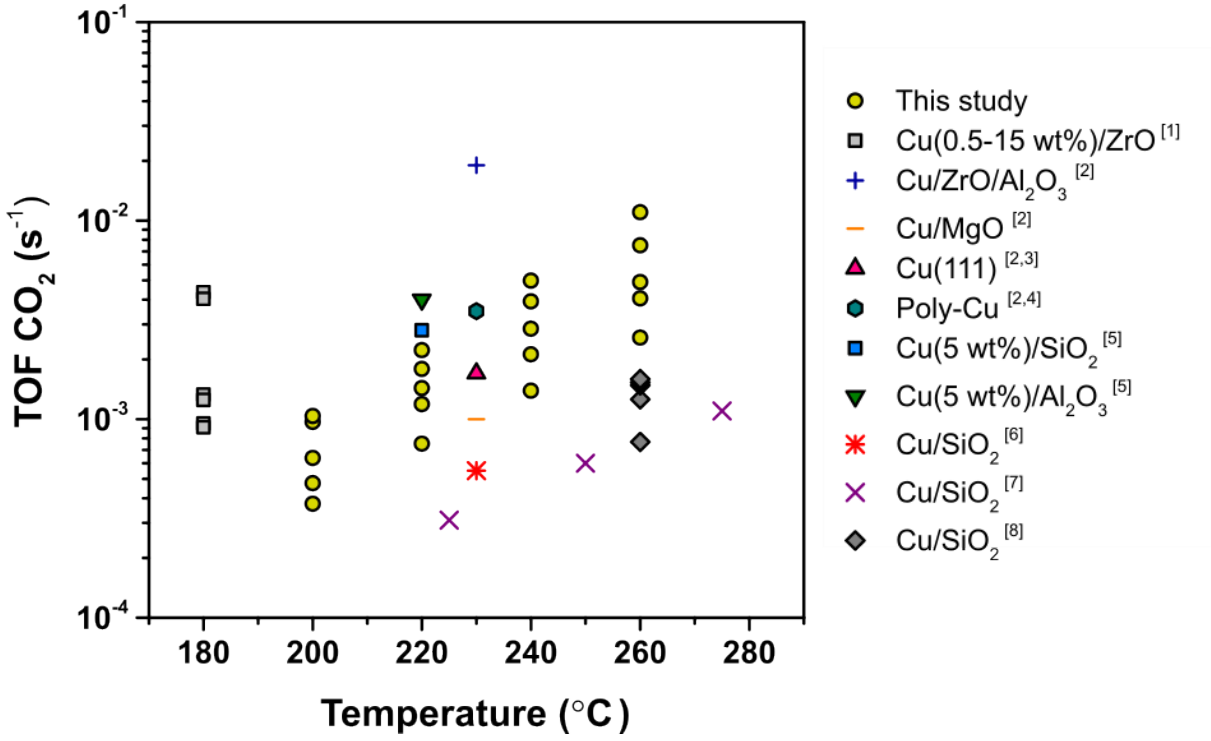

Figure S5 Comparison of CO_2 hydrogenation TOF of this work (yellow symbols) and values reported in literature.

Table S2 Experimental parameter with corresponding literature references for the data reported in Figure S5.

Catalyst	**T (°C)**	**bar**	**H_2/CO_2 ratio**	**Reference**
Cu(0.5-15 wt.%)/ZnO	180	7	9	1
$Cu/ZnO/Al_2O_3$	230	30	3	2
Cu/MgO				
Cu(111)	230	30	3	2,3
Poly-Cu	230			2,4
$Cu(5\ wt.\%)/SiO_2$	220	30	3	5
$Cu(5\ wt.\%)/Al_2O_3$				
Cu/SiO_2	230	25	3	6
Cu/SiO_2	225-275	7,2	3.3	7
Cu/SiO_2	260	8	3	8

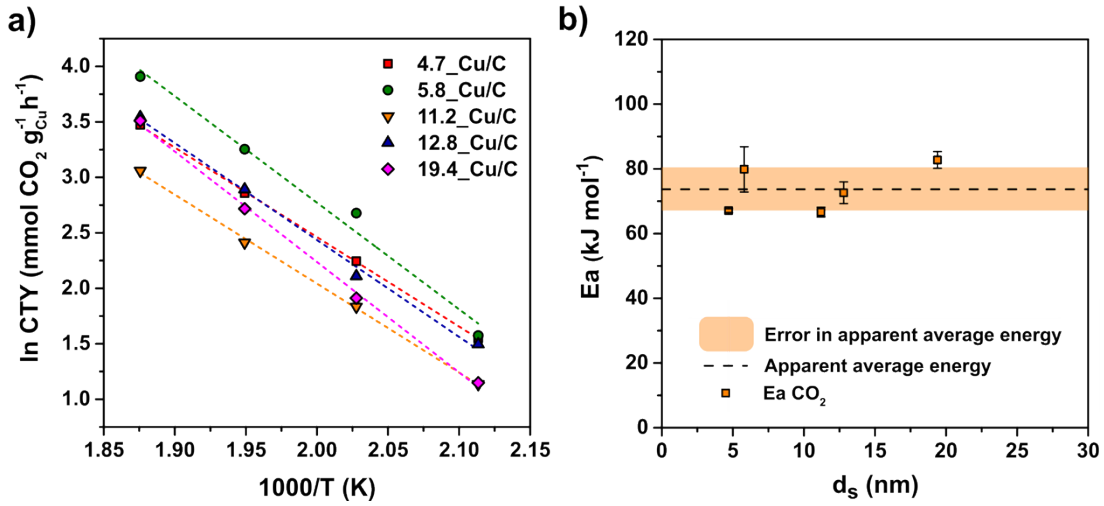

Figure S6 (a) Arrhenius plot with the rate expressed as weight-normalized copper time yield for the whole series of Cu/C catalysts. (b) Apparent activation energy (E_a). Error bars were obtained from the linear fit of the Arrhenius plot. The error on the average E_a was calculated from the standard deviation of the mean with a 95% confidence interval. Reaction conditions: 40 bar(g), 600 mL min^{-1} g_{Cu}^{-1}, H_2/CO_2/He = 67.5/22.5/10 vol%.

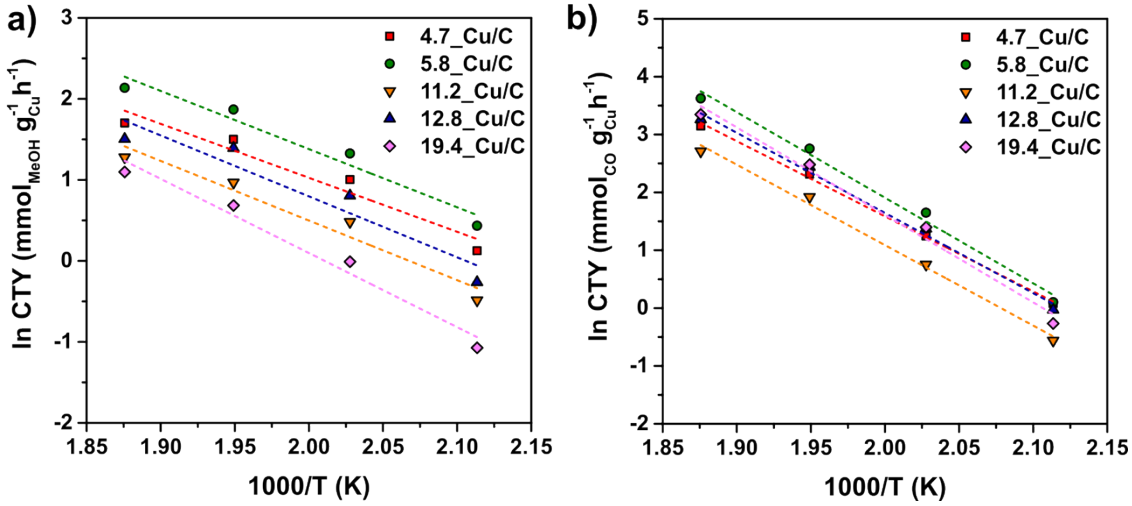

Figure S7 Arrhenius plot (a) for MeOH and (b) CO with the rate expressed as weight-normalized copper time yield for the whole series of Cu/C catalysts.

Table S3 Apparent activation energy for CO_2 conversion, CH_3OH and CO formation.

Name	Ea CO_2 (kJ mol^{-1})	Ea CH_3OH (kJ mol^{-1})	Ea CO (kJ mol^{-1})
4.7_Cu/C	67 ± 1	55 ± 10	108 ± 3
5.8_Cu/C	80 ± 7	60 ± 9	123 ± 8
11.2_Cu/C	67 ± 2	61 ± 10	116 ± 6
12.8_Cu/C	73 ± 3	63 ± 14	115 ± 7
19.4_Cu/C	83 ± 3	76 ± 9	126 ± 10
Average	74 ± 7	63 ± 7	118 ± 6

Section S3: DFT calculations

Based on the computed electronic energies, reaction energies and free energies were calculated at 503 K and 1 bar reference pressure using the results of published calculations.[2] Based on the data on *HCOO/Cu(211) in the supporting information of ref [2], we obtain the following energy differences for the formation of *CHOO/Cu(211) from CO_2(g) and H_2(g): Correction to DFT-energies to improve gas-phase energetics (-0.455 eV), ZPVE contribution (0.169 eV) and finally the Gibbs free energy contribution, including ZPVE (1.238 eV). Based on these contributions, corrected energies and Gibbs free energies for the formation of formate were obtained for all facets by adding -0.286 eV (E) and -0.783 eV (G) to the electronic reaction energies.

Table S4. Unit cell sizes, coverages of different adsorbates on slabs and k-point grids of each calculated systems are depicted.

	HCOO			cis-COOH			CO		
Surfaces	**Unit cell**	**Coverage (ML)**	**k-point sampling**	**Unit cell**	**Coverage (ML)**	**k-point sampling**	**Unit cell**	**Coverage (ML)**	**k-point sampling**
Cu(100)	(4×4)	0.12	3×3×1	(4×4) (3×3)	0.12 0.22	3×3×1 4×4×1	(3×3)	0.11	4×4×1
	(3×3)	0.22	4×4×1	(2×2)	0.5	6×6×1	(2×2)	0.25	6×6×1
	(2×2)	0.5	6×6×1	(3×3) 3×COOH	0.66	4×4×1	(2×2) 2×CO	0.5	6×6×1
	(2×3)	0.66	4×6×1	(2×3) 2×COOH	0.66	4×6×1	-	-	-
	(2×2) 2×HCOO	1	6×6×1	(2×2) 2×COOH	1	6×6×1	(1×1)	1	12×12×1
Cu(110)	(4×4)	0.12	3×3×1	(4×4)	0.12	3×3×1	(3×3)	0.11	4×4×1
	(3×3)	0.22	4×4×1	(3×3)	0.22	4×4×1	(2×2)	0.25	6×6×1
	(2×4) 2×HCOO	0.5	6×3×1	(2×4) 2×COOH	0.5	6×3×1	(2×2) 2×CO	0.5	6×6×1
	(2×2) 2×HCOO	1	6×6×1	(2×2) 2×COOH	1	6×6×1	(1×1)	1	12×12×1
Cu(111)	(4×4)	0.12	3×3×1	(4×4)	0.12	3×3×1	(3×3)	0.11	4×4×1
	(3×3)	0.22	4×4×1	(3×3)	0.22	4×4×1			
	(2×2)	0.5	6×6×1	(2×2)	0.5	6×6×1	(3×3) 2×CO	0.22	4×4×1
	(3×2) 2×HCOO	0.66	4×6×1	(3×2) 2×COOH	0.66	4×6×1	(2×2)	0.25	6×6×1
	(3×3) 3×HCOO	0.66	4×4×1	(3×3) 3×COOH	0.66	4×4×1	(2×2) 2×CO	0.5	6×6×1
	(1×2)	1	12×6×1	(1×2)	1	12×6×1	(1×1)	1	12×12×1
Cu(211)	(3×6)	0.33	4×2×1	(3×6)	0.33	4×2×1	(3×3)	0.33	4×4×1
	(3×4)	0.5	4×3×1	(3×4)	0.5	4×3×1	(3×2)	0.5	4×5×1
	(3×3)	0.66	4×4×1	(3×3)	0.66	4×4×1	(3×3) 2×CO	0.66	4×4×1
	(3×2)	1	4×5×1	(3×2)	1	4×5×1	(3×2) 2×CO	1	4×5×1

Table S5. Total energies of each of the calculated systems. All energies in eV. (a) in x and y direction.

surfaces	**size**[a]	**E**
Cu(100)	4×4	-22.1111
	3×3	-18.003
	2×3	-12.4363
	2×2	-5.5257
	1×1	-1.3813
Cu(110)	4×4	-12.2079
	3×3	-6.8656
	2×4	-6.1029
	2×2	-3.0506
	1×1	-0.7625
Cu(111)	4×4	-26.2532
	3×3	-14.7605
	3×2	-9.8388
	2×2	-6.5573
	1×2	-3.2789
	1×1	-1.6392
Cu(211)	3×6	-28.1207
	3×4	-18.7475
	3×3	-14.0618
	3×2	-9.3660
adsorbates		
Cu(100) - formate	4×4	-44.7658
	3×3	-35.09306
	2×2	-28.10359
	2×3	-53.37807
	2×2 (2×HCOO)	-49.3798
Cu(110) - formate	4×4	-35.1978
	3×3	-29.8633
	2×4 (2×HCOO)	-52.12319
	2×2 (2×HCOO)	-49.0243
Cu(111) – formate	4×4	-48.6733
	3×3	-37.1371
	2×2	-28.9057
	3×2 (2×HCOO)	-54.34907
	3×3 (3×HCOO)	-81.5849
	1×2	-49.5454
Cu(211) – formate	3×6	-51.0394
	3×4	-41.6697
	3×3	-36.98902

	3×2	-32.2313
Cu(100) – cis-COOH	4×4	-43.8454
	3×3	-34.1766
	2×2	-27.2331
	3×3 (3×COOH)	-77.6105
	2×3 (2×COOH)	-51.5739
	2×2 (2×COOH)	-48.3009
Cu(110) – cis-COOH	4×4	-34.1882
	3×3	-28.8539
	2×4 (2×COOH)	-50.14508
	2×2 (2×COOH)	-47.0684
Cu(111) – cis-COOH	4×4	-47.6981
	3×3	-36.1292
	2×2	-28.0289
	3×2 (2×COOH)	-52.7968
	3×3 (3×COOH)	-79.2094
	1×2	-24.0853
Cu(211) – cis-COOH	3×6	-50.0979
	3×4	-40.7196
	3×3	-36.0104
	3×2	-31.2294
Cu(100) - CO	3×3	-25.1395
	2×2	-18.2001
	2×2 (2×CO)	-30.9429
	1×1	-13.4862
Cu(110) - CO	3×3	-19.6398
	2×2	-15.8243
	2×2 (2×CO)	-28.7625
	1×1	-13.3442
Cu(111) – CO	3×3	-27.3015
	3×3 (2×CO)	-39.8089
	2×2	-19.1069
	2×2 (2×CO)	-31.5247
	1×1	-13.1757
Cu(211) – CO	3×3	-26.8508
	3×2	-22.1513
	3×3 (2×CO)	-39.6126
	3×2 (2×CO)	-34.3138

Table S6. Zero-point energy corrections (ZPE), entropy contributions and total energies of gas-phase species and intermediates. (a) All values in eV. (b) $H_{2(g)}$ and $CO_{2(g)}$ are corrected by +0.09 eV and +0.41 eV, respectively, as described in reference [2]. (c) All values from reference [2], that is data based on Cu(211) and the BEEF-vdW functional.

intermediates	E	ZPE[c]	S[c]	C_pdT[c]
HCOO*	see Table S5	0.624	0.000751	0.105
CO*	see Table S5	0.192	0.000452	0.085
Gas-phase species				
$H_{2(g)}$[b]	-7.072	0.270	0.001380	0.091
$CO_{2(g)}$[b]	-18.003	0.320	0.002263	0.098
$CO_{(g)}$	-12.074	0.130	0.02092	0.091

References

1. A. Karelovic and P. Ruiz, *Catal. Sci. Technol.*, 2015, **5**, 869–881.
2. F. Studt, M. Behrens, E. L. Kunkes, N. Thomas, S. Zander, A. Tarasov, J. Schumann, E. Frei, J. B. Varley, F. Abild-Pedersen, J. K. Nørskov and R. Schlögl, *ChemCatChem*, 2015, **7**, 1105–1111.
3. J. Yoshihara, S. C. Parker, A. Schafer and C. T. Campbell, *Catal. Letters*, 1995, **31**, 313–324.
4. T. Fujitani, I. Nakamura, T. Uchijima and J. Nakamura, *Surf. Sci.*, 1997, **383**, 285–298.
5. D. B. Clarke and A. T. Bell, *J. Catal.*, 1995, **154**, 314–328.
6. K. Larmier, W. C. Liao, S. Tada, E. Lam, R. Verel, A. Bansode, A. Urakawa, A. Comas-Vives and C. Copéret, *Angew. Chemie - Int. Ed.*, 2017, **56**, 2318–2323.
7. K. K. Bando, K. Sayama, H. Kusama, K. Okabe and H. Arakawa, *Appl. Catal. A Gen.*, 1997, **165**, 391–409.
8. A. Karelovic, G. Galdames, J. C. Medina, C. Yévenes, Y. Barra and R. Jiménez, *J. Catal.*, 2019, **369**, 415–426.